Proceedings of 12th Cambridge Workshop on Cool Stars, Stellar Systems, & The Sun, 2003 University of Colorado.

Stellar Intrinsic Radial Velocity Noise: Causes and Possible Cures

S. H. Saar[1], A. Hatzes[2], W. Cochran[3], D. Paulson[3]

Abstract.
We explore the causes and test some possible cures for stellar intrinsic radial velocity noise caused by magnetic activity.

1. Introduction

Line asymmetries and central wavelengths on the Sun are altered in bright active regions (AR) in complex ways, probably due to magnetic constriction of convective motions (Livingston 1982; Cavallini et al. 1985; Brandt & Solanki 1990). The integrated effect for the Sun is small, but for active stars, large variations in line asymmetries and the apparent radial velocity (v_r) could result. Starspots can also induce variable line asymmetries and associated v_r perturbations Δv_r (Saar & Donahue 1997; Hatzes 1999). Among other things, these Δv_r sources add noise to v_r searches for exoplanets, limiting the ability to find lower mass and more distant planets. Here, we explore several aspects of the effects of stellar activity on v_r.

2. Data and Observations

We focused on Lick exo-solar planet survey data after ≈ 11/1994 which has the highest v_r precision (internal standard deviation $\sigma_i \approx 3-5$ m s^{-1}; Butler et al. 1996). The 8662Å line of the Ca II infrared triplet (IRT), also present, was measured in a 1Å bandpass relative to the local continuum to generate an $S_{\rm IR}$ value analogous to the Mount Wilson program's $S_{\rm HK}$ (Saar & Cuntz 2001).

We have also begun analysis of very high resolution ($\lambda/\Delta\lambda$ ∼200,000), high S/N (>300) echelle spectra from the 2-D coudé of the 2.7m at McDonald Observatory. Targets were observed both with and without a temperature stabilized I_2 cell to obtain high quality line bisectors and high precision v_r, respectively (Hatzes et al. 1998). The spectra cover ≈18 orders spanning ∼20Å each, centered at ≈5800Å. Bisectors were determined by computing, for each point, a "twin" at the same depth on the other side of the line center using cubic splines; errors were computed following Gray (1988). We selected largely blend-free Fe

[1]Harvard-Smithsonian Center for Astrophysics

[2]Thüringer Sternwarte, Tautenberg

[3]Dept. of Astronomy, U. of Texas, Austin

I lines from Rutten & van der Zalm (1984), and measure a median bisector displacement $v_{\rm med}$ relative to line center (interpolated by a polynomial fit to the line core) for each line. Since line bisectors depend on line strength, wavelength, and excitation (Asplund et al. 2000) we only compare lines with themselves when studying changes.

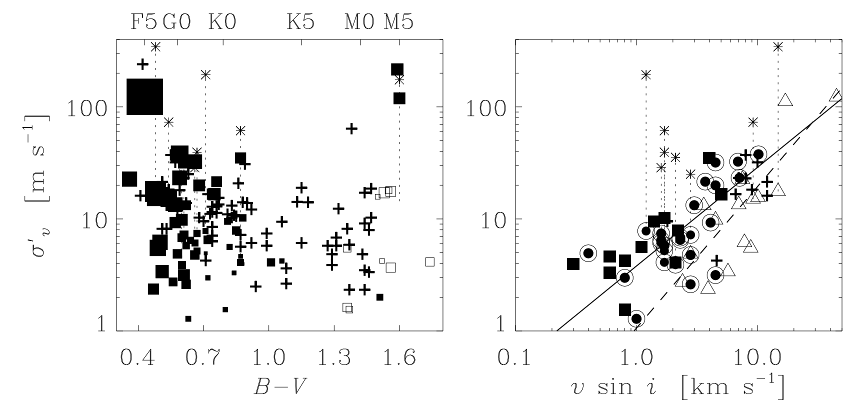

Figure 1. Left: The weighted radial velocity dispersion in excess of the measurement noise, σ'_v, from the Lick $v_{\rm r}$ database, versus $B-V$ color (spectral types at top). The symbol area for Lick stars is $\propto v \sin i$ ($v \sin i$ upper limits are open symbols). Stars with planets are plotted twice, before ($*$) and after removal of the planet orbit and connected (dashed line). Hyads from the Keck survey (+) agree with the Lick data and extend it in the mid-late K/early M stars. Right: σ'_v vs. $v \sin i$, for F ($\triangle$) G ($\odot$) and K (box) Lick survey stars; other symbols as before. Power law fits with $\sigma'_v \propto (v \sin i)^{0.8}$ in G and K stars (solid) and $\sigma'_v \propto (v \sin i)^{1.3}$ in F stars (dashed) are also shown.

3. Analysis and Results

We have redone the Saar et al. (1998) analysis of the rms v_r noise in the Lick survey (first removing the internal measurement noise; i.e., $\sigma'_{v_r} = [\sigma_v^2 - \sigma_i^2]^{0.5}$). The time series we studied spans $\sim$ 5 years (two more than in the Saar et al.). We also have added early results of the Keck Hyades survey (Hatzes & Cochran 2000) which has a similar v_r precision ($\approx$3 m s^{-1}); Hyads with clear companions/trends were not included. We find correlations similar to Saar et al. between σ'_{v_r} and $B-V$, $v \sin i$, the rotation period $P_{\rm rot}$, and normalized Ca II HK emission $R'_{\rm HK}$ (see Figs. 1 and 2). Specifically, we find $\sigma'_{v_r} \propto (v \sin i)^a$, where a =0.83 for GK stars and 1.32 for F stars ($\sigma_{\rm fit}$ = 0.28 and 0.33 dex, respectively); $\sigma'_{v_r} \propto (R'_{\rm HK})^b$ where b =1.1 for GK stars and 1.7 for F stars; and $\sigma'_{v_r} \propto (P_{\rm rot})^c$ where c =-0.97 for GK stars and -1.44 for F stars ($\sigma_{\rm fit}$ = 0.25 and 0.43 dex, respectively). Here F stars are more poorly fit since few have directly measured

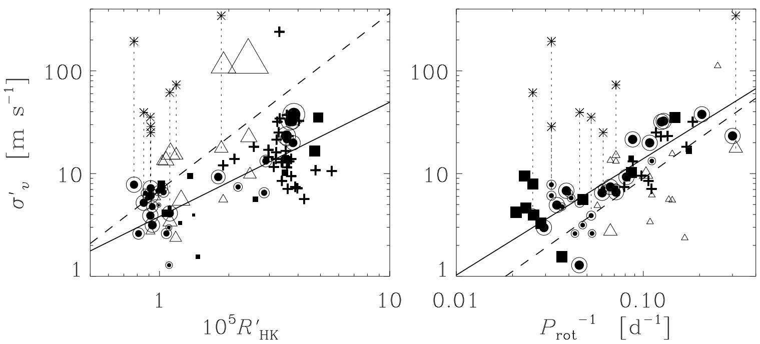

Figure 2. Left: σ'_v vs. $R'_{\rm HK}$; symbols as in Fig. 1 right; symbol size $\propto v \sin i$ for Lick stars. Power law fits with $\sigma'_v \propto (R'_{\rm HK})^{1.1}$ in G and K stars (solid) and $\sigma'_v \propto (R'_{\rm HK})^{1.7}$ in F stars (dashed) are also shown. Right: σ'_v vs. $P_{\rm rot}$; stars with $P_{\rm rot}$ estimated from $R'_{\rm HK}$ plotted at half size. Fits yield $\sigma'_v \propto P_{\rm rot}^{-1.0}$ in G and K stars (solid) and $\sigma'_v \propto P_{\rm rot}^{-1.4}$ in F stars (dashed). The Hyads (+) agree with the $R'_{\rm HK}$ and $P_{\rm rot}$ relations of the Lick stars.

$P_{\rm rot}$. The new relations show slightly higher scatter than in Saar et al. (1998), probably because the longer v_r time series now spans a larger fraction of the typical range of long-term variability/magnetic cycle. The Hyades data agree very well with the trends seen in the Lick data, and clarify the σ'_{v_r} minimum in mid-to-late K and early M stars. Thus, even relatively active stars in this spectral range are good targets for planet searches (typically $\sigma'_v \leq 13$ m s^{-1}).

Long timescale changes in plage coverage will lead to changes in the mean bisector shape and hence the apparent v_r. Saar & Fischer (2000) studied $S_{\rm IR}$ - v_r correlations with an aim towards finding methods of correcting v_r for activity variations. Later work (Saar & Cuntz 2001) revealed a weak ≈1 year periodicity buried in the $S_{\rm IR}$ data used in Saar & Fischer (2000). We have now removed this signal (which is possibly due to a seasonal modulation in the spectrograph's scattered light), and reanalyzed the data, fitting $v_r = \alpha S_{\rm IR} + \beta$. For a "successful" correction, we demanded the probability of significant χ^2 improvement $p_{\chi^2} > 95\%$, $n > 6$, and $|\alpha| > \sigma_\alpha$. Removing the spurious annual signal improves the average v_r correction possible by this method from 45% to 57% of the total σ'_{v_r} (Fig. 3 left). The fraction of successfully corrected stars drops somewhat though, from 29% to 22% of the Lick planet survey sample (suggesting a few of the previous correlations were due to the spurious periodicity). The successfully corrected stars are mostly inactive, or active but with distinct longterm activity trends/cycles. While no new planets have been identified yet, in several cases, apparent periodogram peaks disappeared after applying the $S_{\rm IR}$-based correction to the v_r timeseries. This suggests that activity-based correction of v_r timeseries is already useful, "cleaning" periodograms of some non-planetary signals.

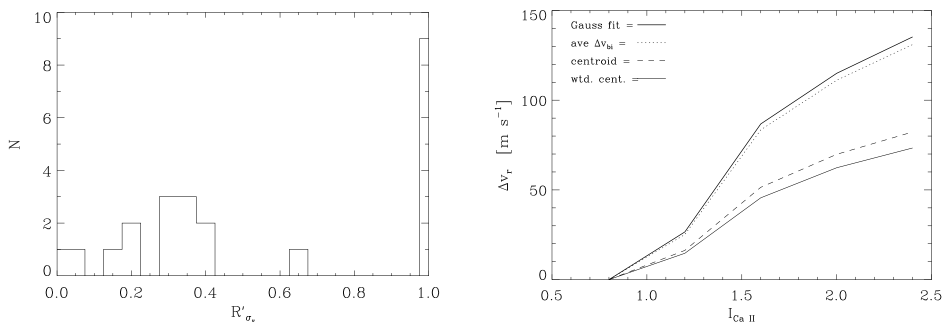

Figure 3. Left: Histogram of the fractional improvement in σ_v above σ_i, R'_{σ_v} (binned by 0.05) in the Lick survey stars after removing linear v_r - $S_{\rm IR}$ trends. 22% of the survey stars are successfully corrected, with $\langle R'_{\sigma_v} \rangle = 45\%$. Right: Maximum v_r perturbation (measured by four methods; see text) due to plage as a function of Ca II emission $I_{\rm CaII}$ at disk-center on a G2 dwarf.

To further explore the effects of plage on v_r, we took observations of solar line bisectors in quiet and active regions with varying Ca II emission levels $I_{\rm CaII}$ (Immerschitt & Schröter 1989) and used these to "warp" model profiles for G2 stars. For this initial study, we considered Gaussian intensity profiles at disk-center, and use several methods to determine the v_r of our "warped" model lines (Gaussian fits, $v_r \approx v_{\rm med}$, line centroid, flux weighted centroid). The maximum velocity perturbation Δv_r (Fig. 3 right) is given by the apparent v_r change between a plage profile and one from a quiet area ($I_{\rm CaII} = 0.8$) We find Δv_r (near disk center) can range up to ~100 m/s, depending on $I_{\rm CaII}$ and the v_r method. Changes in $I_{\rm CaII}$ (due to cycles, active region evolution, and/or rotation) can thus generate large apparent Δv_r at disk center.

Note that v_r - activity correlations will not remove short-term (e.g., rotational) variations in v_r: an identical plage rotated $\pm\theta$ from disk-center have the same observed activity level but opposite signs of Δv_r (Saar & Fischer 2000). To remove such short-term Δv_r, we turn to line bisector variations (e.g., Fig. 4). We have made a preliminary analysis of the limited McDonald data in hand, and find some evidence for correlations between median line bisector displacement and radial velocity v_r. Figure 4 (right) shows mean Δv_r and $\Delta v_{\rm med}$ values for two G0 stars with different activity and $v \sin i$: β Comae ($v \sin i = 4.3$ km s^{-1}; $S_{\rm HK}$=0.201) and 59 Vir ($v \sin i = 7.1$ km s^{-1}; $S_{\rm HK}$=0.313). The data are sparse, but 59 Vir appears to show a larger change in $\Delta v_{\rm med}$ for a given change in Δv_r than β Com, consistent with the idea that bisectors spans are magnified by $v \sin i$ (e.g., Gray 1986). We expect Δv_r - $\Delta v_{\rm med}$ relations will also vary with spectral type (which affects convection and average spottedness).

The combination of short and long-term v_r correction schemes give hope that v_r noise due to activity can eventually be corrected, permitting detection of lower mass and more distant planets around inactive stars, and easing detection of planets around more active stars.

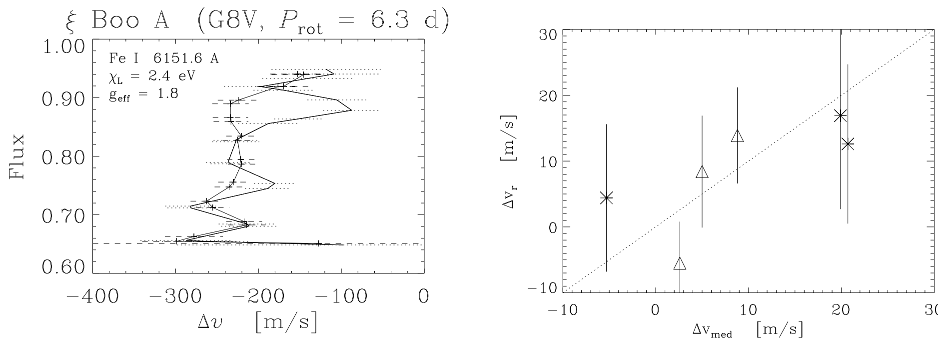

Figure 4. Left: Line bisectors for $\lambda6151$ from $\mathcal{R} = 2{\times}10^5$ McDonald 2-D Coude spectra (S/N = 400 - 550); Δv is set = 0 in the line core. The bisectors (solid and dark solid), taken $\Delta\phi \approx 0.5$ apart in rotational phase, show systematic differences above the errors (horizontal lines). The v_r difference Δv_r and change in the median bisector velocity displacement $\Delta v_{\rm med}$ are in good agreement (both $\sim$10 m s^{-1}). Right: Δv_r versus $\Delta v_{\rm med}$ (averaged over $\sim$30 lines) for 59 Vir ($*$) and β Comae ($\triangle$), 59 Vir with $\approx$1.5 times the projected rotational velocity of β Comae, appears to show a larger change of $\Delta v_{\rm med}$ for a given $\Delta v_{\rm r}$.

Acknowledgments. This work was supported by NSF grants AST-9731652 (SS) and AST-9808980 (WC,DP) and NASA grants NAG5-10630 (SS) and NAG5-9227 (WC,DP).

References

Asplund, M. et al. 2000, A&A, 359, 729

Brandt, P.N. & Solanki, S.K. 1990, A&A, 231, 221

Butler, R.P. et al. 1996, PASP, 108, 500

Cavallini, F., Ceppatelli, G., & Righini, A. 1985, A&A, 143, 116

Cochran, W.D., Hatzes, A. 2000, SPIE, 4004, 252

Gray, D.F. 1986, PASP, 98, 319

Gray, D.F. 1988, *Lectures on Spectral Line Analysis: F, G, and K Stars* (Arva)

Hatzes, A.P, Cochran, W. D., & Bakker, E. J., 1998, ApJ, 508, 380

Hatzes, A.P. 1999, in IAU Colloq. 170, eds. J.B. Hearnshaw & C.D Scarfe, 259

Immerschitt, S. & Schröter, E.H. 1989, A&A, 208, 307

Livingston, W.C. 1992, Nature, 297, 208

Rutten, R. VandenZalm 1984, A&AS, 55, 171

Saar, S.H., Butler, R.P., & Marcy, G.W. 1998, ApJ, 498, L153 (=SBM)

Saar, S.H., & Cuntz, M. 2001, MNRAS, 325, 55

Saar, S.H., & Donahue, R.A. 1997, ApJ, 485, 319

Saar, S.H., & Fischer, D. 2000, ApJ, 534, L105